Monthly Notices
of the
ROYAL ASTRONOMICAL SOCIETY

Mon. Not. R. Astron. Soc. **424,** 1647–1657 (2012) doi:10.1111/j.1365-2966.2012.21099.x

The cosmological impact of intrinsic alignment model choice for cosmic shear

Donnacha Kirk,[1,2]★ Anais Rassat,[3,4] Ole Host[1] and Sarah Bridle[1]

[1]*Department of Physics & Astronomy, University College London, Gower Street, London WC1E 6BT*
[2]*Astrophysics Group, Blackett Laboratory, Imperial College, Prince Consort Road, London SW7 2BZ*
[3]*LASTRO, Swiss Federal Institute of Technology in Lausanne (EPFL), Observatoire de Sauverny, CH-1290, Versoix, Switzerland*
[4]*Laboratoire AIM, UMR CEA-CNRS-Paris 7, Irfu, SEDI-SAP, Service d'Astrophysique, CEA Saclay, F-91191 Gif s/Yvette, France*

Accepted 2012 April 12. Received 2012 March 22

ABSTRACT

We consider the effect of galaxyintrinsic alignments (IAs) on dark energy constraints from weak gravitational lensing. We summarize the latest version of the linear alignment model of IAs, following a brief note of Hirata & Seljak and further interpretation by Laszlo et al. We show the cosmological bias on the dark energy equation of state parameters w_0 and w_a that would occur if IAs were ignored. We find that w_0 and w_a are both catastrophically biased, by an absolute value of just greater than unity under the Fisher matrix approximation. This contrasts with a bias several times larger for the earlier IA implementation. Therefore, there is no doubt that IAs must be taken into account for future stage III experiments and beyond. We use a flexible grid of IA and galaxy bias parameters as used in previous work and investigate what would happen if the Universe is described by used the latest IA model, but we assumed the earlier version. We find that despite the large difference between the two IA models, the grid flexibility is sufficient to remove cosmological bias and recover the correct dark energy equation of state. In an appendix, we compare observed shear power spectra to those from a popular previous implementation and explain the differences.

Key words: galaxies: evolution – cosmology: observations – large-scale structure of Universe.

1 INTRODUCTION

The gravitational lensing of distant galaxy images has the potential to be a powerful cosmological tool. The lensing effect directly probes the matter distribution as a function of redshift, and thus tells us about the expansion history and growth of structure in the Universe. In this way it allows us to constrain the dark energy equation of state, or whatever is causing the apparent accelerated expansion.

Weak gravitational lensing (WGL) poses a number of tough technical challenges if its true potential is to be exploited. The typical cosmic shear induced on galaxies of interest is of the order of 1 per cent, which is significantly smaller than the intrinsic ellipticity of the galaxies themselves. Of course we, as observers, have no access to the *unlensed* galaxy images so we must treat a population of galaxies statistically to recover the cosmological information contained in the cosmic shear signal. The correlation function of galaxy shapes as a measure of gravitational lensing was first proposed by Kaiser (1992) and first observed by Bacon, Refregier & Ellis (2000), Kaiser, Wilson & Luppino (2000), Wittman et al. (2000) and van Waerbeke et al. (2000). For reviews see Bartelmann & Schneider (2001), Munshi et al. (2008), Refregier (2003) and Hoekstra & Jain (2008).

A naive approach to cosmic shear assumes that the intrinsic distribution of galaxy ellipticities is random across the sky. If this was the case, observed ellipticities on a certain patch of sky could be averaged to recover the cosmic shear, because the intrinsic ellipticity would average to zero. However, it was soon pointed out that this assumption of the random intrinsic ellipticity distribution is unjustified (Croft & Metzler 2000; Heavens, Refregier & Heymans 2000; Catelan, Kamionkowski & Blandford 2001; Crittenden et al. 2001).

In fact galaxies may be expected to align with the large-scale gravitational potentials in which they form so we expect physically close galaxies to be preferentially aligned with each other (known as the intrinsic–intrinsic (II) correlation). Hirata & Seljak (2004) noted an additional negative correlation between foreground galaxies shaped by a particular gravitational potential and background galaxies which are lensed by the same potential [known as the gravitational–intrinsic (GI) correlation] which can be of greater magnitude than the II term.

After the alignment of galaxy ellipticities from linear response to the gravitational potential was proposed as an effect by Catelan et al. (2001) the study was put on a firm analytic footing by the introduction of the linear alignment (LA) model by Hirata & Seljak

★E-mail: drgk@star.ucl.ac.uk

(2004, hereafter HS04). This approach, in which the orientation of galaxies responds linearly to the large-scale gravitational potential in which they form, has become the standard model when including the effects of intrinsic alignments (IAs).

Correlated shears of galaxies have been observed at low redshift, where they can be attributed to IAs, by Brown et al. (2002), and have been measured in galaxies selected to be physically close in Mandelbaum et al. (2006), Hirata et al. (2007), Okumura, Jing & Li (2009), Brainerd et al. (2009) and Mandelbaum et al. (2006). Number density–shear correlations are easier to observe since the random galaxy ellipticity only enters the calculation once, and this has been constrained in Mandelbaum et al. (2006), Hirata et al. (2007), Okumura & Jing (2009), Mandelbaum et al. (2011) and Joachimi et al. (2011).

Hirata et al. (2007) noted that the scale dependence of the signal they measured was better matched to theory if the non-linear matter power spectrum was used in the LA instead of the linear power spectrum implied in HS04. Bridle & King (2007) then used the non-linear matter power spectrum in their cosmological forecast calculations. This approach has been called the non-linear alignment (NLA) ansatz. Schneider & Bridle (2010) attempted a more motivated solution for assigning power to the IA model at small scales through the use of the halo model of galaxy clustering. By design their halo model reproduced the LA model at large scales.

The II contribution to IAs can be taken into account in cosmological analyses by removing galaxies with small physical separation from the analysis e.g. King & Schneider (2002), King & Schneider (2003), Heymans & Heavens (2003) and Takada & White (2004). This was attempted in a real analysis of COSMic evOlution Survey (COSMOS) data in Schrabback et al. (2009) by removing the autocorrelation tomographic bin. An extension of this method for GI was suggested in King (2005) and developed to a sophisticated level in Joachimi & Schneider (2008, 2009). Alternatively, a model may be assumed for all the IA contributions, and the free parameters can be marginalized over, as demonstrated at the Fisher matrix (FM) level in Bridle & King (2007), Bernstein (2009), Joachimi & Bridle (2010), Laszlo et al. (2011) and Kirk et al. (2011), and demonstrated on real data in Kirk, Bridle & Schneider (2010).

The redshift evolution of the IA contributions in the LA model was found to be incorrect due to a mistake in HS04 in the conversion between the primordial potential and the matter power spectrum. This was corrected in a new version of HS04, issued as Hirata & Seljak (2010, hereafter HS10). In addition there is an ambiguity in HS04 as to which cosmological epoch is responsible for the 'imprinting' of galaxy IAs. Most starkly the question is, are IAs frozen in at some redshift of formation or do they evolve with the growth of structure, particularly non-linear clustering on small scales? Blazek, McQuinn & Seljak (2011) note this as an issue in the HS04 approach and estimate its effect on the GI amplitude as of the order of 20 per cent. Laszlo et al. (2011) and Kirk et al. (2011) implement one physically motivated solution to this question (as well as including the redshift evolution correction of HS10) which we adopt in this work.

The result of this evolution in the treatment of IAs is that much useful theoretical and observational work has been conducted using an incorrect implementation of the LA model, using often unjustified treatments of the small-scale seeding of galaxy IAs. In this work our aim is to present basic results for the most up to date implementation of the LA model for IAs. We present angular power spectra for components of the shear–shear ($\epsilon\epsilon$), position–position (nn) and position–shear (nϵ) observables as well as the reduction in constraining power in measuring dark energy caused by a robust treatment of IAs and the biasing of cosmological parameters that results from ignoring IAs or treating them using an old model. Many of these results reproduce previous work in the literature which was conducted using an old implementation of the LA model. Specifically, we reproduce Fig. 1 from Joachimi & Bridle (2010) for the new implementation of the LA model which we hope will act as a reference for those wishing to apply it in the future. Furthermore, we investigate the ability of a flexible parametrization of IAs to compensate for using the old LA model compared to the latest version we summarize here.

This paper is organized as follows. In Section 2 we describe the most up to date implementation of the LA model of IAs, detailing our formalism for shear–shear ($\epsilon\epsilon$), position–position (nn) and position–shear (nϵ) correlations. Section 3 presents the bias on cosmological parameter estimation caused by mistreatment of IAs for the latest model, the old model and an intermediate model; we then conclude in Section 4. In Appendix A, we summarize the history of the LA model and present the major differences between the latest implementation and the previous widely used version.

2 THE LINEAR ALIGNMENT MODEL

In this section we summarize the latest LA model interpretation and its contribution to (i) shear–shear correlation, (ii) position–position correlation and (iii) position–shear cross-correlation.

2.1 Shear–shear correlations, $\epsilon\epsilon$

The LA model for galaxy intrinsic ellipticities was suggested by Catelan et al. (2001) and applied quantitatively by HS04, see Section A below for a more complete history. It assumes that, under gravitational collapse, dark matter forms into tri-axial haloes whose major axis is aligned with the maximum curvature of the large-scale gravitational potential. Elliptical galaxies are expected to trace the ellipticity of their parent haloes, meaning that the ellipticity distribution of a population of elliptical galaxies will be linearly related to the curvature of the gravitational potential, ϕ, via

$$\epsilon_+ = C\left(\partial_y^2 - \partial_x^2\right)\phi \tag{1}$$

$$\epsilon_\times = 2C\partial_y\partial_x\phi, \tag{2}$$

where C is an unknown constant, fixed for our formalism by a normalization given below.

In WGL we are interested in IAs as systematic effects which contaminate a measured cosmic shear signal, specifically the shear–shear power spectrum. The LA model motivates the amplitude of two separate terms which affect our ability to accurately measure cosmic shear. The first II term arises when galaxies are physically close. These galaxies form in the same gravitational potential; hence, their intrinsic ellipticities are preferentially aligned. This produces a spurious positive correlation which adds to the measured cosmic shear signal.

The second GI term becomes important when treating galaxies which are close on the sky but separated in redshift. In this case foreground galaxies will align to a foreground gravitational potential which will itself contribute to the gravitational lensing of the background galaxies. This produces an anticorrelation in observed ellipticities and subtracts from the expected cosmic shear signal.

In terms of projected angular power spectra we can write the measured ellipticity power spectrum, $C_l^{\epsilon\epsilon}$, as a sum of the gravitational

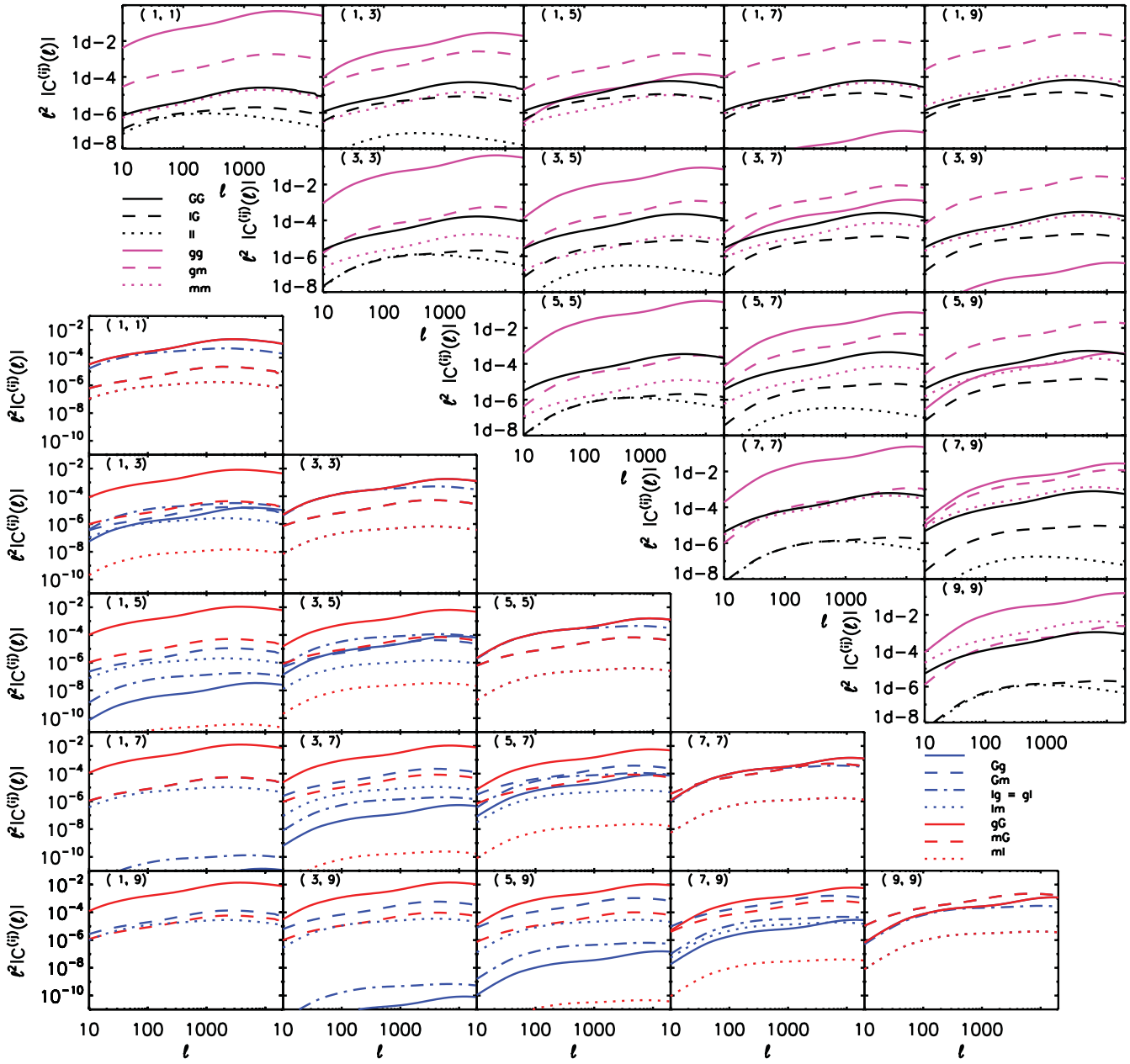

Figure 1. Fiducial power spectra for all correlations considered. The upper-right panels depict the contributions to the $\epsilon\epsilon$ (in black) and nn (in magenta) correlations. The lower-left panels show the contributions to correlations between number density fluctuations and ellipticity. Since we show only correlations $C^{ij}_{\alpha\beta}(l)$ with $i \leq j$, we make in this plot a distinction between nϵ (in red; number density contribution in the foreground, e.g., gG) and ϵn (in blue; number density contribution in the background, e.g. Gg) correlations. In each subpanel a different tomographic redshift bin correlation is shown. For concision only odd bins are displayed. In the upper-right panels the usual cosmic shear signal (GG) is shown as black solid lines; the IA GI term is shown by black dashed lines; the IA II term is shown by dotted black lines; the usual galaxy clustering signal (gg) is shown by magenta solid lines; the cross-correlation between galaxy clustering and lensing magnification (gm) is shown by magenta dashed lines and the lensing magnification correlation functions (mm) are shown by magenta dotted lines. In the lower-left panels the solid blue lines show the correlation between lensing shear and galaxy clustering (Gg); the blue dashed lines show the correlation between lensing shear and lensing magnification (gm); the blue dot–dashed lines show the correlation between IA and galaxy clustering (Ig or equivalently gI); the red solid lines show the correlation between galaxy clustering and lensing shear (gG), which is equivalent to the blue solid lines with redshift bin indices i and j reversed; similarly, the red dashed lines show the correlation between lensing magnification and lensing shear (mG), for cases where the magnification occurs at lower redshift than the shear ($i < j$); finally, the dotted lines show the correlation between lensing magnification and IA (mI).

lensing shear power spectrum and two IA terms:

$$C^{\epsilon\epsilon}(l) = C^{\rm GG}(l) + C^{\rm II}(l) + C^{\rm GI}(l). \quad (3)$$

The cosmic shear power spectrum, $C^{\rm GG}_{ij}(l)$, under the Limber approximation is written as the integrated product of the matter power spectrum, $P_{\delta\delta}(k, \chi)$, and the lensing weight function, $W_i(\chi)$ (Hu 1999),

$$C^{\rm GG}_{ij}(l) = \int_0^{\chi_{\rm hor}} \frac{{\rm d}\chi}{\chi^2} W_i(\chi) W_j(\chi) P_{\delta\delta}(k, \chi), \quad (4)$$

where $P_{\delta\delta}(k, \chi) \equiv P_{\delta\delta}(\frac{l}{f_K(\chi)}, \chi)$, χ is the comoving distance along the line of sight, $f_K(\chi)$ is the comoving angular diameter distance, i, j denote a tomographic redshift bin pair and

$$W_i(\chi) = \frac{3}{2}\frac{H_0^2\Omega_{\rm m}}{c^2}\frac{\chi}{a}\int_{\chi}^{\chi_{\rm hor}} {\rm d}\chi' n_i(\chi')\frac{\chi'-\chi}{\chi'}, \tag{5}$$

with H_0 being the Hubble parameter today, $\Omega_{\rm m}$ the dimensionless matter energy density, c the speed of light, a the dimensionless scale factor and $n_i(\chi')$ the galaxy redshift distribution for a particular bin i.

Similarly, the projected angular power spectra for the IA terms are (HS04)

$$C_{ij}^{\rm II}(l) = \int_0^{\chi_{\rm hor}} \frac{{\rm d}\chi}{\chi^2} n_i(\chi) n_j(\chi) P_{\rm II}(k, \chi) \tag{6}$$

$$C_{ij}^{\rm GI}(l) = \int_0^{\chi_{\rm hor}} \frac{{\rm d}\chi}{\chi^2} W_i(\chi) n_j(\chi) P_{\rm GI}(k, \chi), \tag{7}$$

where, unsurprisingly, the II correlation depends only on the galaxy redshift distribution, $n(\chi)$, while GI depends on the product of the galaxy redshift distribution and the lensing weight function.

The IA 'power spectra', $P_{\rm II}(k, \chi)$ and $P_{\rm GI}(k, \chi)$, are unknown functions of scale and cosmic epoch. In the case of the LA model they become

$$P_{\rm II}(k, \chi) = (-C_1\rho(\chi = 0))^2 P_{\delta\delta}^{\rm lin}(k, \chi = 0) \tag{8}$$

$$P_{\rm GI}(k, \chi) = -C_1\rho(\chi = 0)\sqrt{P_{\delta\delta}^{\rm lin}(k, \chi = 0)}\frac{\sqrt{P_{\delta\delta}(k, \chi)}}{D(z)}, \tag{9}$$

where $P_{\delta\delta}$ is the matter power spectrum, $\rho(\chi = 0)$ is the matter density today and $D(z)$ is the linear growth factor as a function of the redshift z, where it is implicitly meant that $z = z(\chi)$. C_1 is the normalization of the IA contribution and we use a fiducial value of $5 \times 10^{-14}(h^2\,{\rm M}_\odot\,{\rm Mpc}^{-3})^{-1}$, following Bridle & King (2007) who match to the power spectra in HS04 which are based on SuperCOSMOS data from Brown et al. (2002).

The II term is related to the linear matter power spectrum, $P_{\delta\delta}^{\rm lin}$, because we assume that galaxy intrinsic ellipticity is imprinted at the (early) epoch of galaxy formation and subsequently 'frozen in'. As such the power spectrum of its distribution does not undergo the non-linear evolution that the distribution of matter clustering does at late times. The factor of $\sqrt{P_{\delta\delta}^{\rm lin}(k, \chi = 0)P_{\delta\delta}(k, \chi)}/D(z)$ in the GI term reflects the dependence on both the intrinsic ellipticity distribution and the full, late time, mass distribution via gravitational lensing. The exact relation between intrinsic ellipticity, the epoch of galaxy formation and the evolution of galaxy clustering is a vexed and disputed one. A more detailed discussion of the history of the treatment of this relationship can be found in Appendix A, below. We believe that our approach best reflects the physical understanding of the LA model as proposed by HS04 who related the intrinsic ellipticity distribution to the Newtonian potential at the time of galaxy formation.

2.2 Position–position correlations, nn

Any cosmic shear survey provides not only a catalogue of measured galaxy ellipticities but also a record of galaxy positions through their location on the sky and an estimate of their redshift. Analogously to the cosmic shear power spectrum we may define the galaxy position density power spectrum, $C^{\rm nn}(l)$, the Fourier transform of the galaxy position two-point correlation function. It is conceptually useful to divide the contributions up as follows:

$$C^{\rm nn}(l) = C^{\rm gg}(l) + C^{\rm mm}(l) + C^{\rm gm}(l). \tag{10}$$

Here we have separated the contribution from galaxy clustering itself, gg, from the contribution due to lensing magnification, mm, and the cross-correlation of the two, gm. The lensing contribution manifests because a galaxy may increase (or decrease) in size as a result of the image distortion. The application of Liouville's theorem tells us that the process of WGL conserves surface brightness density; hence, a larger (smaller) galaxy will appear brighter (dimmer) due to the lensing effect. For a magnitude limited survey this can affect the statistics of galaxy clustering as otherwise too faint galaxies are promoted into the survey by magnification and vice versa. As the nn correlation is effectively just a counting of galaxies and their relative positions, there is no ellipticity contribution and we can ignore IAs.

The equation for the pure galaxy clustering term is relatively straightforward in the Limber approximation,

$$C_{ij}^{\rm gg}(l) = \int_0^{\chi_{\rm hor}} \frac{{\rm d}\chi}{\chi^2} n_i(\chi) n_j(\chi) b_{\rm g}^2(k, z) P_{\delta\delta}(k, \chi), \tag{11}$$

where the window function is the galaxy redshift distribution as we would expect and we have introduced the galaxy bias term, $b_{\rm g}$, to reflect our understanding that galaxies are a biased tracer of the underlying matter distribution. As before, $P_{\delta\delta}(k, \chi) \equiv P_{\delta\delta}(\frac{l}{f_K(\chi)}, \chi)$. In general $b_{\rm g}$ is an unknown function of scale and cosmic epoch. The details of the galaxy bias formalism we assume in this paper, along with other bias terms, are explained in Section 3 below.

The magnification power spectrum and galaxy clustering-magnification cross-term can be written as

$$C_{ij}^{\rm mm}(l) = 4(\alpha_i - 1)(\alpha_j - 1)C_{ij}^{\rm GG}(l) \tag{12}$$

$$C_{ij}^{\rm gm}(l) = 2(\alpha_j - 1)C_{ij}^{\rm gG}(l), \tag{13}$$

where α_i is defined as the slope of the luminosity function, evaluated at the median redshift of the bin i, and $C^{\rm gG}(l)$ is defined in Section 2.3. In this approach, we are following Joachimi & Bridle (2010). We treat each of the α_i terms as a free parameter in the model and take fiducial parameters from equations 32, 33 and table 2 of Joachimi & Bridle (2010); see Appendix A of that paper for more details.

2.3 Position–shear correlations, nϵ

As well as $\epsilon\epsilon$ and nn correlations themselves, we can cross-correlate the two fields to form the galaxy position–shear, nϵ, cross-correlation functions as first proposed by Hu & Jain (2004) in the context of dark energy. This is often referred to as galaxy–galaxy lensing, in which the mass of a foreground galaxy distorts the shape of a background galaxy. Here we consider the general cross-correlation which includes contributions from larger dark matter structures, from magnification and also from IAs if the correlated galaxies are physically close. We can write the contributions to the full nϵ term as

$$C^{{\rm n}\epsilon}(l) = C^{\rm gG}(l) + C^{\rm gI}(l) + C^{\rm mG}(l) + C^{\rm mI}(l) \tag{14}$$

(Joachimi & Bridle 2010).

The individual expressions for the terms in the $C^{{\rm n}\epsilon}(l)$ expansion contain combinations of quantities already considered,

$$C_{ij}^{\rm gG}(l) = \int_0^{\chi_{\rm hor}} \frac{{\rm d}\chi}{\chi^2} n_i(\chi) W_j(\chi) \\ b_{\rm g}(k, z) r_{\rm g}(k, z) P_{\delta\delta}(k, \chi) \tag{15}$$

$$C_{ij}^{\rm gI}(l) = \int_0^{\chi_{\rm hor}} \frac{{\rm d}\chi}{\chi^2} n_i(\chi) n_j(\chi) \\ b_{\rm g}(k,z) r_{\rm g}(k,z) b_{\rm I}(k,z) r_{\rm I}(k,z) P_{\rm GI}(k,\chi) \quad (16)$$

$$C_{ij}^{\rm mG}(l) = 2(\alpha_i - 1) C_{ij}^{\rm GG}(l) \quad (17)$$

$$C_{ij}^{\rm mI}(l) = 2(\alpha_i - 1) C_{ij}^{\rm GI}(l), \quad (18)$$

where we have introduced the additional free functions $r_{\rm g}$ and $r_{\rm I}$ which appear due to the possible stochastic relation between the galaxy and dark matter distributions (Dekel & Lahav 1999) as discussed in Section 3 below. As before $P_{\delta\delta}(k,\chi) \equiv P_{\delta\delta}(\frac{l}{f_K(\chi)},\chi)$. We note that $P_{\rm GI}(k,\chi)$ appears in the $C_{ij}^{\rm gI}(l)$ term because it describes how the dark matter distribution relates to the IAs, and we assume that the relation between the galaxy distribution and the dark matter distribution can be accounted for by the product $b_{\rm g} r_{\rm g}$.

2.4 Summary of observables and fields

The observables considered in this paper and the different fields which contribute to each observable are summarized in Table 1. In Fig. 1 we plot the angular power spectra of all the considered components for a fiducial stage IV lensing survey. For our fiducial model, in this paper, we use the following survey specification: 20 000 deg^2 with a galaxy number density of 35 arcmin^{-2} and a redshift distribution given by the Smail-type $n(z)$,

$$n(z) = z^\alpha \exp\left(-\left(\frac{z}{z_0}\right)^\beta\right), \quad (19)$$

with $\alpha = 2$, $\beta = 1.5$ and $z_0 = 0.9/\sqrt{2}$, divided into 10 tomographic bins with equal number density out to redshift 3 and normalized so that $\int n(z)\,{\rm d}z = 1$. A Gaussian photometric redshift error of $\sigma_z = 0.05(1+z)$ is assumed with no catastrophic outliers in redshift. We constrain the set of cosmological parameters $\{\Omega_{\rm m}, w_0, w_{\rm a}, h, \sigma_8, \Omega_{\rm b}, n_{\rm s}\}$ which take the values $\Omega_{\rm m} = 0.25$, $w_0 = -1$, $w_{\rm a} = 0$, $h = 0.7$, $\sigma_8 = 0.8$, $\Omega_{\rm b} = 0.05$ and $n_{\rm s} = 1$. All results assume a flat, Λ cold dark matter cosmology. The linear matter power spectrum is calculated using the Eisenstein & Hu (1998) fitting function and non-linear corrections are applied where appropriate using the Smith et al. (2003) formalism.

Fig. 1 is presented and formatted in the same way as fig. 3 in Joachimi & Bridle (2010). The purpose is to supply a new reference plot using the most up to date implementation of the LA model for IAs. All lines which do not include an 'I' term will be identical in both versions of the plot. However, as Joachimi & Bridle (2010) use the original HS04 implementation, from before the publication of the erratum incorporated into HS10, and present lines for the NLA ansatz, there are differences in any lines containing an I contribution. The NLA version of HS04 is the most widely used in the literature to date; we refer to it subsequently as HS04NL. Note that we are employing the NLA prescription in HS04NL even though this was not explicitly discussed in the original HS04 paper. See Appendix A for a more detailed explanation of the evolution of the LA model and the differences between various implementations.

Table 1. Summary of observables considered in this paper and different fields which contribute to each observable.

Observables	
$\epsilon\epsilon$	Shear–shear
nn	Position–position
nϵ	Position–shear
Fields	
G	Gravitational lensing
I	IA
g	Galaxy clustering
m	Cosmic magnification

The upper triangle of Fig. 1 shows the contributions to the shear–shear correlation function in black for every other tomographic bin pairing. As usual the lensing contribution is the largest on all angular scales, but is most dominant in the autocorrelations at high redshift. The II IA term is most important in the autocorrelations and negligible for widely spaced bins. The GI contribution is largest for separated bins (shown as IG for compactness – see the caption). The IA contributions are typically 1 to 10 per cent of the lensing signal.

The contributions to the position–position correlation function are shown in pink in the upper triangle, and as expected, the autocorrelations are dominated by the intrinsic clustering of galaxies. The cross-correlations of separated bins can be dominated by the cross-correlation of galaxy clustering and magnification. As expected, the magnification-only term is most important at high redshift, although it never exceeds the other terms for the redshift ranges we consider.

The lower triangle shows the various contributions to the position–shear cross-correlation function and the effect of reversing the tomographic bin order where relevant (see the caption). The correlation between lensing shear and galaxy clustering is the strongest of these contributions and is largest when the tomographic bins are separated with the galaxies in the foreground. This is the usual galaxy–galaxy lensing contribution. Interestingly, it is still large in the autocorrelations which is due to the galaxies in the nearest part of the redshift bin lensing the galaxies in the farthest part. There is a non-negligible contribution in some of the cross-terms from the lensing of galaxies in a nearer tomographic bin by galaxies in a farther tomographic bin, due to the overlap in redshift distributions (solid blue lines). At highest redshifts the magnification terms start to dominate. The cross-correlation between magnification and IA is mostly one of the smallest terms.

3 BIASING OF COSMOLOGICAL PARAMETERS

The LA model is currently our best description of galaxy IA over a range of cosmologies. It has been shown that ignoring IAs in an analysis can significantly bias the measurement of fundamental cosmological parameters (Bridle & King 2007). In this section we quantify this bias and examine the effect of moving from the old standard LA implementation to the new one. We also explore the bias produced by using the old implementation rather than the new.

A naive approach to cosmic shear measurements would ignore IAs and measure values for cosmological parameters which are systematically biased. By employing a flexible IA model and marginalizing over a set of nuisance parameters we lose precision but hope to produce unbiased cosmological measurements. In this section we quantify the cosmological bias which results from ignoring IAs and also the cosmological bias which results from employing the HS04NL LA model rather than the current LA model.

To this end we employ the cosmological bias formalism of Huterer et al. (2006, see also Amara & Refregier 2007 and

appendix A of Joachimi et al. 2011),

$$\delta p_\alpha = F^{-1}_{\alpha\beta} \sum_l \Delta C_{ij} \left(\mathrm{Cov} \left[C_{ij}(l), C_{\mathrm{mn}}(l) \right] \right)^{-1} \frac{\partial C_{\mathrm{mn}}(l)}{\partial p_\beta}, \qquad (20)$$

where δp_α is the cosmological bias on each parameter considered, C_{ij} are the projected angular power spectra, $\frac{\partial C_{\mathrm{mn}}(l)}{\partial p_\beta}$ are the derivatives of these power spectra with respect to the cosmological parameters, $\mathrm{Cov}\left[C_{ij}(l), C_{\mathrm{mn}}(l)\right]$ is the covariance matrix of the power spectra, calculated according to equation 39 in Joachimi & Bridle (2010), and $F^{-1}_{\alpha\beta}$ is the inverse of the FM for our set of cosmological parameters, calculated as

$$F_{\alpha\beta} = \sum_{l=l_{\mathrm{min}}}^{l_{\mathrm{max}}} \sum_{(i,j),(m,n)} \frac{\partial C_{ij}(l)}{\partial p_\alpha} \mathrm{Cov}^{-1} \left[C_{ij}(l), C_{\mathrm{mn}}(l) \right] \frac{\partial C_{\mathrm{mn}}(l)}{\partial p_\beta}.$$

Each of the FM terms is calculated using the assumed IA model. ΔC_{ij} is the difference between the data vector calculated using the assumed model and the true model,

$$\Delta C_{ij} = C^{\mathrm{assumed}}_{ij}(l) - C^{\mathrm{true}}_{ij}(l). \qquad (21)$$

Fig. 2 shows the cosmological bias on the dark energy equation of state parameters if IAs are assumed not to exist but they are truly present according to one of the following: the HS04NL implementation; the new model; or an intermediate between the two, called HS10NL. The bias is the distance between the centre of the 'true' contour [−1,0] and the centre of the contours which assume no IAs.

Note that the bias parametrization used is based on the FM formalism which assumes purely Gaussian errors in the parameters and observables which respond linearly with respect to the parameters in question. The parametrization is very likely to break down for parameter values more than $\sim 2-3\sigma$ away from the fiducial cosmology. As such the more extreme bias values seen in Figs 2 and 3 should not be read as exact. What they can tell us is rough relative bias between different scenarios and it is clear that any scenario producing an absolute bias on w_0 of order unity or above can be considered to be 'catastrophically biased'. For clarity we use the notation σ_{FM} when quoting the size of biases on parameters with respect to the errors on the unbiased constraints to remind the reader that they are calculated assuming that the FM formalism is valid.

The intermediate model (HS10NL) is introduced to disentangle the two effects which change between HS04NL and the new LA implementation. It includes the correct factors of a, introduced by HS10 and shown in equation (A5), but it always applies the non-linear matter power spectrum, $P^{\mathrm{lin}}_{\delta\delta}(k, z)$, to the IA terms, following the Bridle & King (2007) interpretation of HS04NL. So this HS10NL model applies the correct redshift evolution to IAs but assumes that the effects of non-linear clustering are always present, even in the II term, by adopting the NLA ansatz.

Ignoring IAs causes strong biasing on the dark energy parameters, no matter which IA model is assumed to be true. The new implementation is the least biased at $\sim 8\sigma_{\mathrm{FM}}$ away from the true model. However, ignoring IAs appears to still bias w_0 by of the order of ~ 1.5. The HS10NL model is more biased at $\sim 20\sigma_{\mathrm{FM}}$. The HS04NL implementation produces the strongest cosmological bias, with the contour far outside the plotted area. At a point this

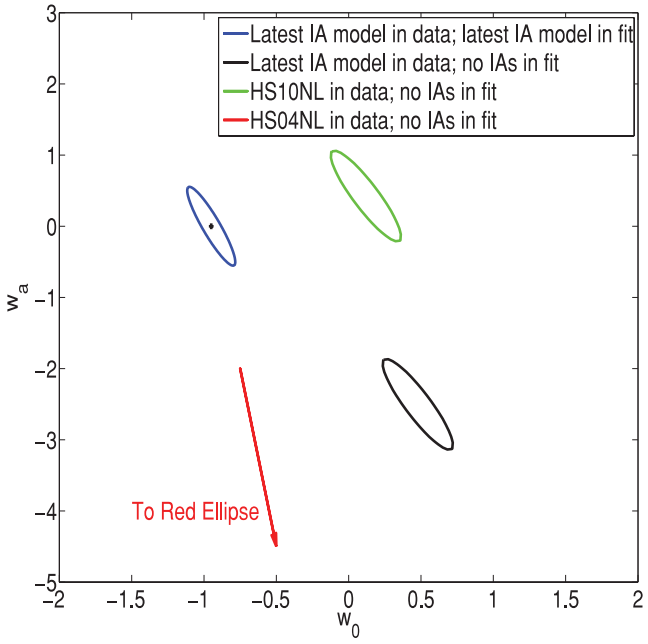

Figure 2. 95 per cent confidence limits on the dark energy parameters w_0 and w_{a} for the IA implementation from this work (blue contour) and the biased constraints if it is assumed that IAs do not exist but in fact the new implementation (black contour), the HS10NL implementation (green contour) or the HS04NL implementation (off plot, direction indicated by red arrow) is true. The cosmological bias is given by the offset between each displaced contour and the fiducial values of (−1, 0) (black cross). Results are presented for an observable data vector of shear–shear ($\epsilon\epsilon$) correlations only. It is assumed that we enjoy perfect knowledge of the IA contribution for each implementation.

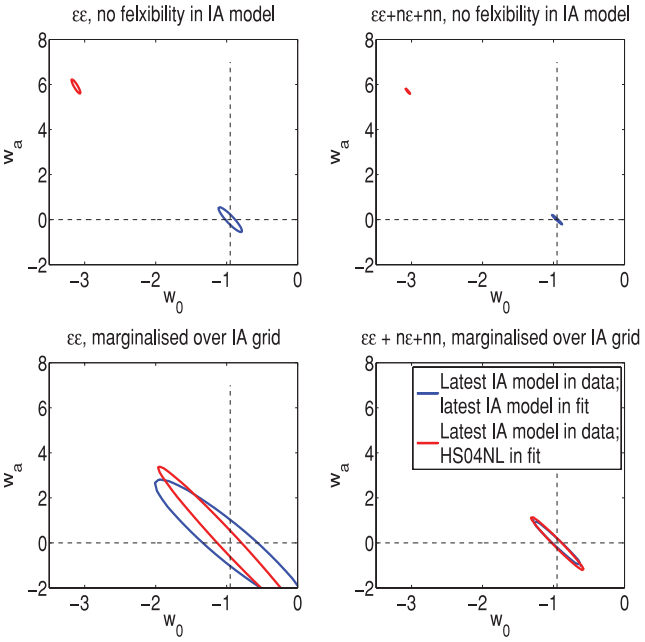

Figure 3. 95 per cent confidence limits on the dark energy parameters w_0 and w_{a} for the IA implementation from this work (blue contours) and the biased constraints if the old HS04NL implementation is assumed (red contours). The cosmological bias is given by the offset between the displaced contour and the fiducial values of (−1, 0) (black dotted lines). Results are presented for an observable data vector of shear–shear ($\epsilon\epsilon$) correlations alone (left-hand panels) and the full combination of shear–shear, shear–position and position–position ($\epsilon\epsilon + \mathrm{n}\epsilon + \mathrm{nn}$) correlations (right-hand panels). Each probe combination is shown for the case of perfect knowledge of IAs and galaxy bias (top panels) and for the case where our ignorance is accounted for by marginalization over the nuisance parameter grid with $N_k = N_z = 7$ (bottom panels).

far away from the fiducial parameter values the Gaussian assumptions of the FM and bias formalisms certainly break down and it would be wrong to put much faith in the exact direction/distance of the predicted bias. What is clear however is that the effect is very strong. This finding is what we would expect given that the move from HS04NL to the new implementation has reduced the impact of IAs, not only through changes to their redshift evolution, but also through the removal of IA power on small scales.

The general biasing trend is the same when we calculate for a stage III type survey, like the Dark Energy Survey, with biases of $\sim 4\sigma_{\rm FM}$ for the latest model, $\sim 8\sigma_{\rm FM}$ for the HS10NL implementation and $\sim 30\sigma_{\rm FM}$ for the HS04NL model.

So far we have not taken into account any uncertainty in the IA model, but assumed that they are zero in the parameter fitting, whichever model we employ to describe them in the true model. In reality, we are aware that our knowledge of IAs from simulations and observations is still developing and relatively uncertain. The case is similar for galaxy bias, introduced in Section 2.2 and employed below. To parametrize our ignorance of both effects and their cross-correlations we use a grid of nuisance parameters

$$X = A_X Q_X(k, z), \tag{22}$$

where A_X is a constant amplitude parameter, free to vary about a fiducial value of 1, and $Q_X(k, z)$ is a grid of $N_k \times N_z$ nodes logarithmically spaced in k/z space, each of which is allowed to vary independently around a fiducial value of 1. A final smooth grid is created by spline interpolation over the values of the grid nodes. For more details of this nuisance parameter grid see Joachimi & Bridle (2010), Laszlo et al. (2011) and Kirk et al. (2011). This was inspired by the marginalization of Bernstein (2009) which led to the grid implementation in Joachimi & Bridle (2010).

We define four sets of nuisance parameters which each take the form of this grid,

$$b_{\rm I}(k, z) = A_{b_{\rm I}} Q_{b_{\rm I}}(k.z) \tag{23}$$

$$b_{\rm g}(k, z) = A_{b_{\rm g}} Q_{b_{\rm g}}(k.z) \tag{24}$$

$$r_{\rm I}(k, z) = A_{r_{\rm I}} Q_{r_{\rm I}}(k.z) \tag{25}$$

$$r_{\rm g}(k, z) = A_{r_{\rm g}} Q_{r_{\rm g}}(k.z). \tag{26}$$

The 'b' terms can be understood as bias terms between the power spectrum of a field X and the matter power spectrum, i.e.

$$\frac{P_{XX}(k, z)}{P_{\delta\delta}(k, z)} = b_X^2(k, z), \tag{27}$$

and the 'r' terms are biasing terms which arise in cross-correlations, i.e.

$$\frac{P_{XY}(k, z)}{P_{\delta\delta}(k, z)} = b_X(k, z) r_X(k, z) b_Y(k, z) r_Y(k, z). \tag{28}$$

The 'b' and 'r' terms are both functions of the clustering and stochastic bias as described in Dekel & Lahav (1999).

These sets of nuisance parameters then appear, in different combinations, in each angular power spectrum integral where galaxy clustering, g, or the IA term, I, appear:

$$C_{ij}^{\rm II}(l) = \int \frac{{\rm d}\chi}{\chi^2} n_i(\chi) n_j(\chi) b_{\rm I}^2(k, z) P_{\rm II}(k, \chi) \tag{29}$$

$$C_{ij}^{\rm GI}(l) = \int \frac{{\rm d}\chi}{\chi^2} W_i(\chi) n_j(\chi) b_{\rm I}(k, z) r_{\rm I}(k, z) P_{\rm GI}(k, \chi) \tag{30}$$

$$C_{ij}^{\rm gg}(l) = \int \frac{{\rm d}\chi}{\chi^2} n_i(\chi) n_j(\chi) b_{\rm g}^2(k, z) P_{\delta\delta}(k, \chi) \tag{31}$$

$$C_{ij}^{\rm gG}(l) = \int \frac{{\rm d}\chi}{\chi^2} n_i(\chi) W_j(\chi) b_{\rm g}(k, z) r_{\rm g}(k, z) P_{\delta{\rm G}}(k, \chi) \tag{32}$$

$$C_{ij}^{\rm gI}(l) = \int \frac{{\rm d}\chi}{\chi^2} n_i(\chi) n_j(\chi) b_{\rm I}(k, z) r_{\rm I}(k, z) \, b_{\rm g}(k, z) r_{\rm g}(k, z) P_{\delta{\rm I}}(k, \chi), \tag{33}$$

while nuisance parameters appear in $c_{ij}^{\rm gm(}{}_{l)}$ and $c_{ij}^{\rm mI(}{}_{l)}$ due to their dependence on $c_{ij}^{\rm gG(}{}_{l)}$ and $c_{ij}^{\rm GI(}{}_{l)}$, respectively. In general this means that, for the full suite of observables $\epsilon\epsilon + {\rm n}\epsilon + {\rm nn}$, we marginalize over a total of $4(1 + N_k \times N_z)$ nuisance parameters, plus 30 that parametrize the magnification effects. As before $P_{\delta\delta}(k, \chi) \equiv P_{\delta\delta}(\frac{l}{f_K(\chi)}, \chi)$. When we employ the nuisance grid in this work we set $N_k = N_z = 7$, giving a total of 230 nuisance parameters. This follows the practice used in Joachimi & Bridle (2010) for the purposes of comparison (see their table 2). We also restrict the information used in the galaxy field to linear scales as in Rassat et al. (2008).

This current paper presents the most advanced interpretation of the LA model. However, most of the work on IAs in the literature has been conducted using a non-linear version of the original interpretation presented in HS04. In Fig. 3 we quantify the bias introduced on the dark energy parameters from the use of this HS04NL approach rather than the latest implementation introduced in this work. When the IA signals (whether from the old or new models) are assumed to be known perfectly there is a very strong biasing effect which would result in a very worrying systematic mismeasurement of cosmology.

In the case where $\epsilon\epsilon$ correlations alone are considered, the bias is $\sim 25\sigma_{\rm FM}$ of the constraining power of the cosmic shear signal given the true IA contribution. When the full set of correlations including position information, $\epsilon\epsilon + {\rm n}\epsilon + {\rm nn}$, are considered this biasing increases to $\sim 65\sigma_{\rm FM}$. As previously discussed, when the effect is this strong the exact position/direction of the biasing is likely to be well outside the competence of the FM-based formalism but the fact that there is a very significant effect should not be doubted.

When we employ the robust parametrization of both IA and galaxy bias uncertainties via the grid of nuisance parameters described above we see a striking change in the results. As we would expect the constraining power of either probe combination decreases as we have marginalized over 130 free parameters which represent our ignorance of the exact details of IAs (and another 100 for galaxy bias). What is also clear is that the biasing of our cosmological estimates has decreased to well within the 1σ error of the respective probes.

The constraints on w_0 and $w_{\rm a}$ from the full $\epsilon\epsilon + {\rm n}\epsilon + {\rm nn}$ combination after marginalization over 230 nuisance parameters are only reduced by a factor of 2 compared to the naive (and heavily biased if the wrong IA model is used) constraints from $\epsilon\epsilon$ alone when it is assumed that IAs are perfectly known. This corresponds to a factor of 2.6 reduction in DETF figure of merit (Albrecht et al. 2006).

4 CONCLUSIONS

Galaxy IAs are the most important astrophysical systematic in the study of cosmic shear. As increasing volumes of data become available from WGL surveys more interest is being paid to their correct treatment. Much of this work has been dominated by the LA model, originally introduced in HS04 (and the NLA extension which we refer to as HS04NL). This original implementation was subsequently corrected in HS10 and detailed attention paid to the

treatment of non-linear clustering in Laszlo et al. (2011) and Kirk et al. (2011).

However, much of the existing literature has been produced using the uncorrected HS04NL model. In this paper we have provided a brief explanation of the evolution of, and context surrounding, the LA model for IAs, highlighting the most important differences between the HS04NL model and the latest implementation.

We have calculated the angular power spectra of the cosmic shear observables, correcting the implicit mistake of Joachimi & Bridle (2010), which was based on HS04, which we hope will act as a new reference for those interested in applying IAs to their cosmic shear analysis.

The main motivation for the study of IAs is the measurement of unbiased constraints of key cosmological parameters. We show that the new LA implementation significantly reduces the impact of IAs, and hence the bias, but that the effect is still very significant, producing a bias at the tens of σ level when we assume perfect knowledge of IAs.

If we did know the IA signal perfectly then we could produce unbiased measurements by simply subtracting the IA signal from our measured cosmic shear. In practice, it is useful to parametrize our ignorance of the true IA signal through a set of nuisance parameters which are marginalized over to produce weaker but hopefully unbiased cosmological estimates. We show that a robust grid of 130 nuisance parameters for IAs and magnification uncertainties, allowed to vary in scale and redshift, effectively removes the bias due to assuming an incorrect IA model.

The same effect holds when our observables are extended to include shear–shear, position–position and shear–position correlations. The extra observables increase constraining power so that we are able to produce unbiased constraints on $\epsilon\epsilon + \mathrm{n}\epsilon + \mathrm{nn}$ which recover 40 per cent of the constraining power of the highly biased constraint from $\epsilon\epsilon$ alone when the wrong IA model is assumed.

The LA model has allowed a firm foothold on the study of IAs to develop over the last decade. We have detailed an updated implementation of the most used IA model and its physical motivation, showing a reduction in biasing of cosmological constraints. In addition, we reiterate that a robust nuisance parameter model can control the biasing due to IAs for either the old or new implementations. Together, these results should give us confidence that the IA effect is under control as we begin to analyse the first data from large cosmic shear surveys.

However, our somewhat pessimistic approach carries the cost of reduced constraining power. Future work, focused on accurate simulation and measurement of IAs, is sure to provide more detail on the physical mechanisms responsible for the initial intrinsic ellipticity distribution and its evolution. This better knowledge of IAs will improve our ability to model them and reduce our dependence on brute-force marginalization over nuisance parameters. As such the marginalized constraints which we present in Fig. 3 may be a worst-case scenario. With better knowledge of IAs, better constraints on cosmology will be possible.

ACKNOWLEDGMENTS

The authors are very grateful to Lisa Voigt who was intimately involved as a contributor to the preparatory work leading to this paper. The authors are thankful to Benjamin Joachimi for useful discussions regarding Joachimi & Bridle (2010). They also thank Rachel Bean and Istvan Laszlo for very useful discussion and work on the best implementation of the LA model. SB acknowledges support from the Royal Society in the form of a University Research Fellowship and the European Research Council in the form of a starting grant with number 240672. This research is in part supported by the Swiss National Science Foundation (SNSF).

REFERENCES

Albrecht A. et al., 2006, preprint (arXiv:0609591)
Amara A., Refregier A., 2007, 381, 1018
Bacon D., Refregier A., Ellis R., 2000, 318, 625
Bartelmann M., Schneider P., 2001, Phys. Rep., 340, 291
Bernstein G. M., 2009, ApJ, 695, 652
Blazek J., McQuinn M., Seljak U., 2011, J. Cosmol. Astropart. Phys., 5, 10
Brainerd T. G., Agustsson I., Madsen C. A., Edmonds J. A., 2009, preprint (arXiv:0904.3095)
Bridle S., King L., 2007, New J. Phys., 9, 444
Brown M. L., Taylor A. N., Hambly N. C., Dye S., 2002, MNRAS, 333, 501
Buergers J., van de Hulst H., ed., 1951, Proc. Joint Symp., Motion of Gaseous Masses of Cosmical Dimensions. Paris, Aug 1949, Central Air Documents Office, Dayton
Catelan P., Kamionkowski M., Blandford R. D., 2001, MNRAS, 320, L7
Ciotti L., Dutta S. N., 1994, MNRAS, 270, 390
Crittenden R. G., Natarajan P., Pen U.-L., Theuns T., 2001, ApJ, 559, 552
Croft R. A. C., Metzler C. A., 2000, ApJ, 545, 561
Dekel A., Lahav O., 1999, ApJ, 520, 24
Doroshkevich A. G., 1970, Afz, 6, 581
Eisenstein D. J., Hu W., 1998, ApJ, 496, 605
Heavens A., Peacock J., 1988, MNRAS, 232, 339
Heavens A., Refregier A., Heymans C., 2000, MNRAS, 319, 649
Heymans C., Heavens A., 2003, MNRAS, 339, 711
Heymans C., Brown M., Heavens A., Meisenheimer K., Taylor A., Wolf C., 2004, MNRAS, 347, 895
Hirata C. M., Seljak U., 2004, Phys. Rev. D, 70, 063526 (HS04)
Hirata C. M., Seljak U., 2010, preprint (arXiv:astro-ph/0406275) (HS10)
Hirata C. M. et al., 2004, MNRAS, 353, 529
Hirata C. M., Mandelbaum R., Ishak M., Seljak U., Nichol R., Pimbblet K. A., Ross N. P., Wake D., 2007, MNRAS, 381, 1197
Hoekstra H., Jain B., 2008, Annu. Rev. Nuclear Part. Sci., 58, 99
Hu W., 1999, ApJ, 522, L21
Hu W., Jain B., 2004, Phys. Rev. D, 70, 043009
Huterer D., Takada M., Bernstein G., Jain B., 2006, MNRAS, 366, 101
Jing Y. P., 2002, MNRAS, 335, L89
Joachimi B., Bridle S. L., 2010, A&A, 523, A1
Joachimi B., Schneider P., 2008, A&A, 488, 829
Joachimi B., Schneider P., 2009, A&A, 507, 105
Joachimi B., Mandelbaum R., Abdalla F. B., Bridle S. L., 2011, A&A, 527, A26
Kaiser N., 1992, ApJ, 388, 272
Kaiser N., Wilson G., Luppino G. A., 2000, ApJ, submitted (astro.ph/0003338)
King L., Schneider P., 2002, A&A, 396, 411
King L. J., 2005, A&A, 441, 47
King L. J., Schneider P., 2003, A&A, 398, 23
Kirk D., Bridle S., Schneider M., 2010, MNRAS, 408, 1502
Kirk D., Laszlo I., Bridle S., Bean R., 2011, preprint (arXiv:1109.4536)
Laszlo I., Bean R., Kirk D., Bridle S., 2011, preprint (arXiv:1109.4535)
Mackey J., White M., Kamionkowski M., 2002, MNRAS, 332, 788
Mandelbaum R., Hirata C. M., Broderick T., Seljak U., Brinkmann J., 2006, MNRAS, 370, 1008
Mandelbaum R. et al., 2011, 410, 844
Munshi D., Valageas P., Van Waerbeke L., Heavens A., 2008, Phys. Rep., 462, 67
Okumura T., Jing Y. P., 2009, ApJ, 694, L83
Okumura T., Jing Y. P., Li C., 2009, ApJ, 694, 214
Peebles P. J. E., 1969, ApJ, 155, 393
Rassat A. et al., 2008, preprint (arXiv:0810.0003)
Refregier A., 2003, Ann. Rev. Astron. Astrophys., 41, 645
Schaefer B. M., 2009, Int. J. Mod. Phys. D, 18, 173

Schneider M. D., Bridle S., 2010, MNRAS, 402, 21275
Schrabback T. et al., 2010, A&A, 516, A63
Sciama D. W., 1955, MNRAS, 115, 3
Smith R. E. et al., 2003, MNRAS, 341, 1311
Takada M., White M., 2004, ApJ, 601, L1
van den Bosch F. C., Abel T., Croft R. A. C., Hernquist L., White S. D. M., 2002, ApJ, 576, 21
van Waerbeke L. et al., 2000, A&A, 358, 30
White S. D. M., 1984, ApJ, 286, 38
Wittman D. M., Tyson J. A., Kirkman D., Dell'Antonio I., Bernstein G., 2000, Nat, 405, 143

APPENDIX A: HISTORY OF THE LA MODEL

The history of galaxy IA studies goes back to Buergers and van de Hulst (1951) and Sciama (1955) who discussed that galaxies may acquire angular momentum through tidal torquing, in which anisotropic shear flows distort the protogalaxy and lead to a local rotation. The theory was further developed analytically by Peebles (1969), Doroshkevich (1970) and White (1984), and first simulated by Heavens & Peacock (1988). If galaxy orientations are correlated with their angular momenta, then we may expect neighbouring galaxies to be aligned (e.g. van den Bosch et al. 2002). Heavens et al. (2000), Croft & Metzler (2000) and Catelan et al. (2001) simultaneously pointed out that this could lead to a contaminating term in WGL, and this was investigated further in Crittenden et al. (2001), Mackey, White & Kamionkowski (2002), Jing (2002), Heymans et al. (2004), Hirata et al. (2004) and Bridle & King (2007). See Schaefer (2008) for a more recent review.

Ciotti & Dutta (1994) described a second ansatz to motivate the IAs of elliptical galaxies, based on tidal stretching of the host halo by the surrounding large-scale structure. Catelan et al. (2001) showed that the correlation function of the IAs should be proportional to that of the tidal field and thus be significant even on large scales. This contrasts with the correlation function expected from tidal torque theory which has a higher order dependence on the tidal field and thus decays more rapidly.

Heavens et al. (2000) and Croft & Metzler (2000) used the shapes of dark matter haloes in N-body simulations as a proxy for elliptical galaxy shapes and estimated the possible contamination to the (then) recent cosmic shear detections. They found the contamination to be a fraction of the measured signal but Heavens et al. (2000) commented that low-redshift surveys would be strongly affected and Croft & Metzler (2000) point out that future tomographic measurements will also be significantly affected.

HS04 discussed both models and used the term 'linear alignment model' to describe the alignment of the galaxy halo with the tidal stretch of the local gravitational potential. Previous to HS04 the cosmic shear contamination was believed to come from physically close galaxies due to both galaxies forming in the same large-scale structure. HS04 identified a second term due to the IA of one galaxy near to a large mass which would correlate with the gravitational alignment of a distant galaxy lensed by the same mass. The first of these two was labelled 'intrinsic-intrinsic' (II) correlation and the second 'gravitational-intrinsic' (GI) correlation.

Following the approach of Catelan et al. (2001), HS04 assume that galaxy intrinsic ellipticity follows the linear relation

$$\gamma^{\rm I} = -\frac{C_1}{4\pi G}\left(\Delta_x^2 - \Delta_y^2, 2\Delta_x\Delta_y\right)\mathcal{S}[\Phi_P], \tag{A1}$$

where Φ_P is the Newtonian potential at the time of galaxy formation, smoothed by some filter $\mathcal{S}$ that cuts off fluctuations on galactic scales, G is the Newtonian gravitational constant, Δ is a comoving derivative and C_1 is a normalization constant.

After relating the primordial potential to the linear matter power spectrum, HS04 calculate the II and GI power spectra

$$P_{\rm II}^{\rm HS04}(k,\chi) = \left(\frac{-C_1\bar{\rho}(z)}{\bar{D}(z)}\right)^2 P_{\delta\delta}^{\rm lin}(k,\chi) \tag{A2}$$

$$P_{\rm GI}^{\rm HS04}(k,\chi) = -\frac{C_1\bar{\rho}(z)}{\bar{D}(z)} P_{\delta\delta}^{\rm lin}(k,\chi) \tag{A3}$$

in terms of the linear theory matter power spectrum at comoving distance χ corresponding to the redshift z, $P_{\delta\delta}^{\rm lin}(k,\chi)$. Here $\bar{\rho}(z)$ is the mean density of the Universe and $\bar{D}(z) = (1+z)D(z)$ is the rescaled growth factor $D(z)$.

Note that HS04 actually present the power spectra for $\tilde{\gamma}_{\rm I}$, the density weighted intrinsic shear (and δ, $\tilde{\gamma}_{\rm I}$ for the GI term). This is because galaxies are not randomly positioned, but are expected to form preferentially in regions of higher matter density. This leads to higher order terms in the IA power spectra which are usually ignored because they are about an order of magnitude smaller than the leading term in the above equations (Bridle & King 2007).

These equations were used in several publications until the discovery of missing factors of a^2 which arose in the conversion factor between the density perturbation and the primordial potential. These were corrected in an erratum of HS10. In the updated version, equations (A2) and (A3) become

$$P_{\rm II}^{\rm HS10}(k,\chi) = \left(\frac{-C_1\bar{\rho}(z)}{\bar{D}(z)}a^2\right)^2 P_{\delta\delta}^{\rm lin}(k,\chi) \tag{A4}$$

$$P_{\rm GI}^{\rm HS10}(k,\chi) = -\frac{C_1\bar{\rho}(z)}{\bar{D}(z)}a^2 P_{\delta\delta}^{\rm lin}(k,\chi). \tag{A5}$$

Originally HS04 related their $P_{\rm II}$ and $P_{\rm GI}$ to the linear matter power spectrum $P_{\delta\delta}^{\rm lin}$. It was subsequently indicated by Hirata et al. (2007) that more power at small scales may fit the data better and Bridle & King (2007) proposed that the non-linear matter power spectrum be substituted for the linear in what became known and the NLA model, which was then applied in Bridle & King (2007), Schneider & Bridle (2010), Mandelbaum et al. (2011), Joachimi et al. (2011), Kirk et al. (2010), Laszlo et al. (2011) and Kirk et al. (2011). It is this common NLA approach which we describe as HS04NL,

$$P_{\rm II}^{\rm HS04NL}(k,\chi) = \left(\frac{-C_1\bar{\rho}(z)}{\bar{D}(z)}\right)^2 P_{\delta\delta}(k,\chi) \tag{A6}$$

$$P_{\rm GI}^{\rm HS04NL}(k,\chi) = -\frac{C_1\bar{\rho}(z)}{\bar{D}(z)} P_{\delta\delta}(k,\chi); \tag{A7}$$

the non-linear matter power spectrum is used in both equations.

In this work we employ a more physically motivated approach based on the idea that galaxy IAs are seeded at some early epoch of galaxy formation and do not evolve with redshift. This was the original intent of the LA model in Catelan et al. (2001) and HS04. This principle is apparent from the original HS04 equations by the presence of the $1/D(z)$ terms which divide out the growth. Therefore, we relate our II term directly to $P_{\delta\delta}^{\rm lin}$ but the GI term picks up some contribution from the later (linear and non-linear) growth of large-scale structure via its dependence on cosmic shear. This is included in the formalism by the geometric mean of the linear and non-linear matter power spectra in equation (9). This was proposed and discussed further in Laszlo et al. (2011) and Kirk et al. (2011).

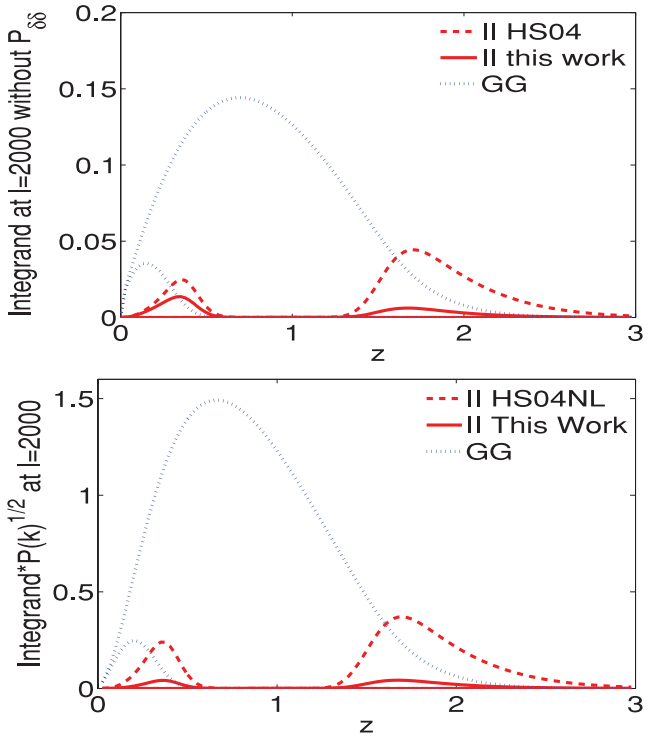

Figure A1. Integrand of the GG angular power spectrum at a multipole of $l = 2000$ ($2\pi G\rho(z)a^2c^{-2}W_i(\chi)\sqrt{P_{\delta\delta}(k,\chi)}$) (blue dotted) and the II integrand for the original HS04 LA model ($C_1\rho(z)an_i(\chi)\sqrt{P_{\delta\delta}(k,\chi)}$) (red dotted) and the LA model given in this work ($C_1\rho(z=0)n_i(\chi)\sqrt{P^{\rm lin}_{\delta\delta}(k,\chi)}$) (red solid), both shown for $l = 2000$. We present integrands without (upper panel) and with the appropriate matter power spectrum term (lower panel). Each angular power spectrum is plotted for the first and tenth tomographic redshift bins of our fiducial survey; these appear to the left and right hand of each plot, respectively. Here the term $P(k)$ corresponds to either the linear or non-linear matter power spectrum depending on the term (G or I) and on the implementation used (HS04NL or this work).

Note that equations (A6) and (A7) are the same as our expressions in equations (8) and (9) with the pre-factor in brackets simplified, and there is a different treatment of the linear/non-linear matter power spectra.

An improvement on the contributions at non-linear scales was developed by Schneider & Bridle (2010) by developing a halo model of IAs. We do not use it here as it does not contain full flexibility of the cosmological model.

In this paper we discuss and illustrate the difference between the models, summarized in Fig. A1. The changes can be divided into two types: (i) the correct use of the a^2 terms as included in HS10 and (ii) the consistent use of the linear matter power spectrum for the II correlation but the square root product of the linear and non-linear power spectra for the GI correlation (see equation 9). The upper panel of Fig. A1 includes only the first change by plotting the square root of the C_l integrand without the contribution from the matter power spectrum. The terms plotted for bins $i = 1, 10$ are

$$\text{GG}: \quad \frac{2\pi G\rho(z)a^2}{c^2}W_i(\chi) \tag{A8}$$

$$\text{II}^{\text{HS04}}: \quad C_1\rho(z)an_i(\chi) \tag{A9}$$

$$\text{II}^{\text{this work}}: \quad C_1\rho(z=0)n_i(\chi). \tag{A10}$$

The lower panel includes the square root of the matter power spectrum contribution, plotting

$$\text{GG}: \quad \frac{2\pi G\rho(z)a^2}{c^2}W_i(\chi)\sqrt{P_{\delta\delta}(k,\chi)} \tag{A11}$$

$$\text{II}^{\text{HS04NL}}: \quad C_1\rho(z)an_i(\chi)\sqrt{P_{\delta\delta}(k,\chi)} \tag{A12}$$

$$\text{II}^{\text{this work}}: \quad C_1\rho(z=0)n_i(\chi)\sqrt{P^{\rm lin}_{\delta\delta}(k,\chi)}. \tag{A13}$$

Correct inclusion of the a^2 terms produces an IA signal which is constant with redshift, rather than the one which increases with redshift in the HS04NL prescription. IAs are normalized against a C_1 value measured at low redshift, which means that the new II term is comparable to the HS04NL term at low redshift (if it were possible to show the II terms at $z = 0$ on the top panel of Fig. A1 they would be identical) but increasingly diverges at higher redshifts. This is why the II kernel for the 10th (high-z) redshift bin is reduced more as we move from HS04NL to the new model than the equivalent lines for the first (low-z) bin. The shear–shear term is unaffected by our treatment of IAs, which means that IAs make a less significant contribution to the total shear signal at higher redshift than in the HS04NL approach.

The impact of moving from the common NLA approach to our motivated treatment of non-linear clustering and IAs is to weaken the contribution of IAs relative to cosmic shear because we discard all non-linear clustering power for the IA terms. This means we lose all power due to non-linear clustering in the II term and half the non-linear power from the GI term where the I contribution is linear but the G contribution remains dependent on the fully non-linear matter power spectrum. The impact is felt at all redshifts but the effect is strongest at low z where non-linear clustering is strongest. Fig. A2 shows the projected angular power spectra for those components which are affected by the change from the HS04NL model (as used in Joachimi & Bridle 2010) to the latest implementation described in this work. The format of the plot is the same as Fig. 1; lines corresponding to the latest LA implementation are thick versions of the same line style as their HS04NL equivalents. The shear–shear (GG) angular power spectra are, of course, unaffected by the change; they are shown in the upper triangle for comparison.

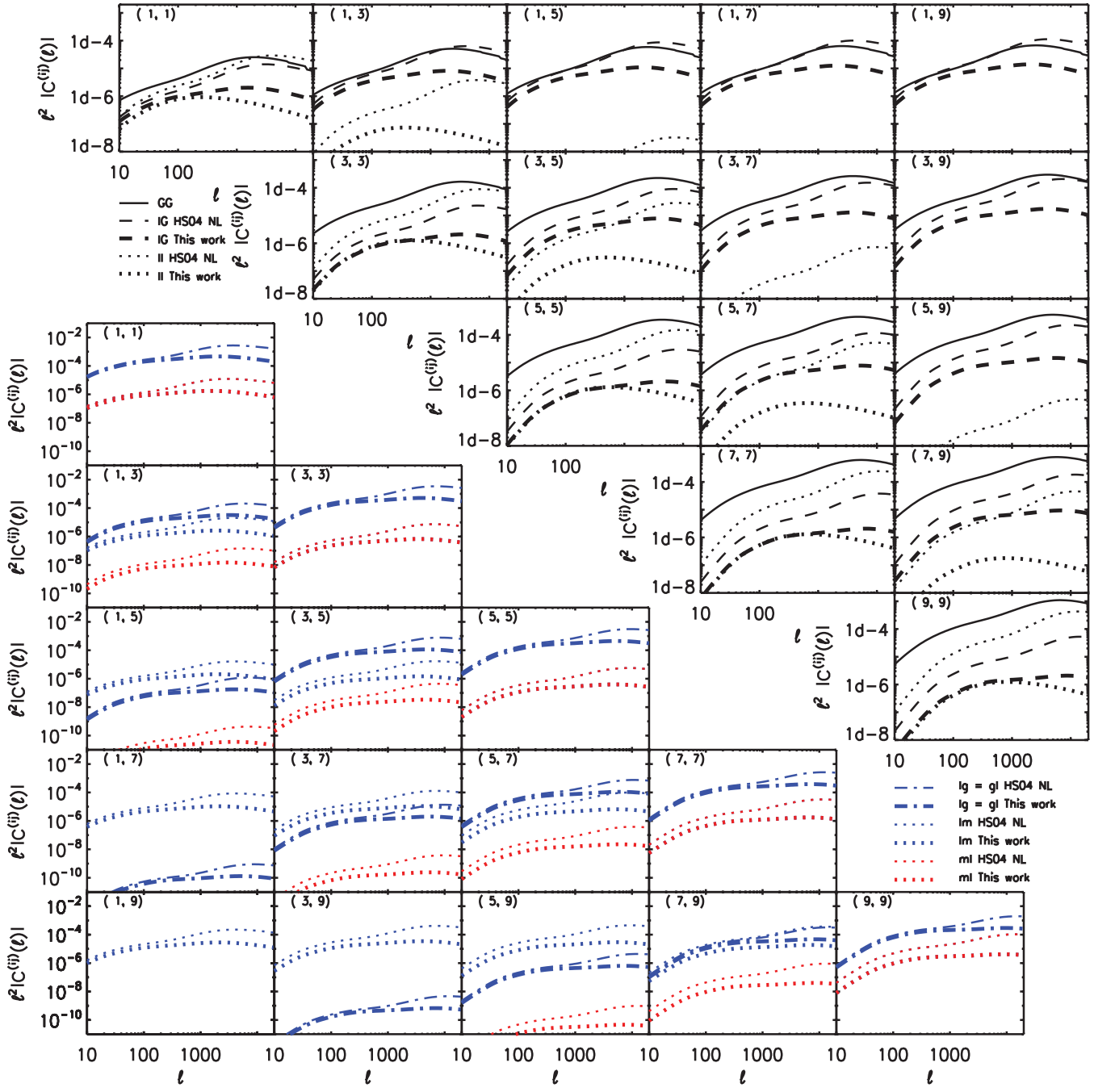

Figure A2. Projected angular power spectra which contain IA contributions. Computed for our fiducial survey and displayed for a variety of tomographic redshift bin combinations as in Fig. 1. Power spectra are computed using the HS04NL approach (narrow lines) and the new approach described in this work (thick lines). The GG (solid black narrow) power spectrum is shown for comparison.

This paper has been typeset from a TEX/LATEX file prepared by the author.